CURRENT CLASSIFICATION STRATEGIES BASED ON THE TRANSFER FUNCTION AND FIELD QUALITY OF THE NEW SUPERCONDUCTING MAGNETS IN THE HL-LHC*

A. Fornara†, M. Giovannozzi, G. Sterbini
CERN, Meyrin, Switzerland

Abstract

Precise optics control around the main interaction regions of the HL-LHC is essential to reach the target values of β^* and the collider's nominal performance, while maintaining sufficient beam aperture and satisfying machine protection constraints. The field quality of the high-luminosity insertion-region magnets is particularly critical for the accelerator performance, possibly impacting the achievable integrated luminosity. In this context, magnet sorting strategies, i.e. the allocation of a compatible slot in the tunnel based on the actual magnet properties, such as the transfer function and magnet field quality, can provide an effective handle to improve both linear and non-linear optics performance of the upgraded insertion regions. This work focuses on the Q2 magnets of the HL-LHC inner triplets, which are built at CERN and for which sorting remains a feasible option, as it is compatible with production and installation schedules. The effectiveness and trade-offs of these approaches are studied using a combination of analytical calculations and full HL-LHC lattice simulations. The studies resulted in an effective sorting recommendation, which is adopted for the installation of the Q2 magnets.

INTRODUCTION

When building accelerator magnets, deviations of the field quality (FQ) compared to the ideal magnet design are unavoidable due to manufacturing tolerances. The detrimental effects of these magnetic field imperfections can be alleviated by appropriately choosing the positions of the magnets in the accelerator lattice, since different optical conditions can reduce the sensitivity to such errors. This strategy, known as sorting, has been investigated during the design phase of several modern accelerators (see e.g. Refs. [1–11]) and successfully applied in the CERN LHC [12–14]. Ideally, a sorting scheme relies on a large pool of magnets, from which subsets are selected and optimally assigned to the most suitable positions in the ring. In this context, the LHC main dipoles, consisting of 1232 magnets, provided an excellent test case for sorting methods. From a theoretical perspective, an effective sorting procedure requires a robust figure of merit to assess any given magnet distribution, together with an efficient algorithm to scan the large space of possible magnet permutations. From a hardware perspective, sorting is demanding in terms of magnet storage capacity (to allow large samples of magnets to be available simultaneously) and in terms of early magnetic measurements, which must be carried out while the magnets are still compatible with many potential locations in the ring. In general [15], these requirements impose stringent constraints on construction, testing, and installation schedules, which may not always be feasible, and in such circumstances the benefits of sorting are significantly reduced.

Similarly to LHC, sorting is foreseen for the new insertion magnets of the LHC luminosity upgrade (HL-LHC) [16]. In this case, however, the magnet families (triplet quadrupoles and separation/recombination dipoles) to be installed during the upcoming Long Shutdown 3 (planned roughly from mid-2026 to mid-2030) consist of only a limited number of units (16 quadrupole cryostats). Nevertheless, it is expected that sorting can still provide a beneficial performance margin for the accelerator by mitigating natural beta-beating, arising from variations in the triplet quadrupole transfer functions, and by improving beam lifetime through better minimisation of integrated non-linear aberrations. Any sorting strategy for HL-LHC magnets must also take into account the tight scheduling constraints. In this paper, we present and discuss the status of the sorting studies for the Q2 triplet quadrupoles manufactured at CERN, extending previous analyses presented in Ref. [17]. We note that other sorting activities for HL-LHC magnets are reported in Ref. [18].

Q2 MAGNET SPECIFICATIONS

The inner triplets of the HL-LHC comprise eight MQXFB magnets (Q2 type), arranged in Q2A/Q2B pairs across the four sides of the two high-luminosity insertion regions, namely IR1 and IR5 (see [19, Fig. 2]). In each pair, Q2A denotes the unit closer to the interaction point (IP), and the two magnets are powered in series.

At the time of this study, four magnets had already been paired and assigned to fixed installation slots, based on the analysis of the measured transfer function (TF): MQXFB03 (Q2A) with MQXFB06 (Q2B) on the right side of IR1 (R1) and MQXFB05 (Q2A) with MQXFB04 (Q2B) on the left side of IR5 (L5). The remaining four units, MQXFB07, MQXFB08, MQXFB10, and MQXFB11, required the sorting into the two available slots, R5 and L1. The magnetic properties relevant to sorting are listed in Table 1. At the time of writing, the FQ of MQXFB11 was not measured at cold yet. Therefore, for this magnet, the b_4 value is extrapolated from warm measurements.

The four magnets to be sorted were already configured as two Q2A units (MQXFB07, MQXFB11) and two Q2B units (MQXFB08, MQXFB10). Four options are therefore

* Work supported by the HL-LHC project.
† andrea.fornara@cern.ch

Table 1: MQXFB magnet properties relevant for sorting. All values are from cold measurements (apart from MQXFB11, for which b_4 was extrapolated from warm). The reference radius for the b_4 measurements is $R_{\mathrm{ref}} = 50$ mm.

Magnet	Type	Slot	TF [T/kA]	b_4 [u]
MQXFB03	Q2A	R1	58.571	+0.92
MQXFB06	Q2B	R1	58.523	+0.22
MQXFB05	Q2A	L5	58.700	+0.79
MQXFB04	Q2B	L5	58.655	−0.25
MQXFB07	Q2A	TBD	58.563	+0.81
MQXFB08	Q2B	TBD	58.594	−0.09
MQXFB10	Q2B	TBD	58.643	−0.38
MQXFB11	Q2A	TBD	58.502	−0.21

possible, taking into account IR-side assignements and pairings between magnets. Option 1 (MQXFB11-MQXFB10 in L1 and MQXFB07-MQXFB08 in R5) and Option 4 (MQXFB07-MQXFB08 in L1 and MQXFB11-MQXFB10 in R5) pair magnets whose TF values are close to each other. Option 2 (MQXFB11-MQXFB08 in L1 and MQXFB07-MQXFB10 in R5) and Option 3 (MQXFB07-MQXFB10 in L1 and MQXFB11-MQXFB08 in R5), conversely, result in larger TF imbalances within each pair.

SIMULATION SETUP

All simulations are performed on the HL-LHC lattice [20] using the Xsuite tracking framework [21]. The lattice is configured at the top energy with round optics ($\beta^* = 0.15$ m), fractional tunes $Q_x = 0.31$, $Q_y = 0.32$, and a half crossing angle $\theta_c/2 = 0\,\mu$rad. This configuration is representative of the early commissioning stage of the collision optics.

TF-based sorting proceeds as follows: A reference $\beta^0_{x,y}$ is computed from the ideal lattice. The measured TF errors are then applied to the Q2 magnets for a given sorting option. Tunes and chromaticities are rematched to their nominal values. Finally, the perturbed $\beta_{x,y}$ is evaluated to obtain the β-beating associated with the given option: $\Delta\beta_{x,y}/\beta_{x,y} = (\beta_{x,y} - \beta^0_{x,y})/\beta^0_{x,y}$.

For the analysis based on b_4, the procedure is extended by installing the measured octupolar field errors as thin multipoles in the lattice and by calculating the amplitude detuning generated by these errors.

TRANSFER FUNCTIONS SORTING

The β-beating induced by the TF errors for all four options are shown in Fig. 1 for Beam 1. The results for Beam 2 (not shown) yields nearly identical conclusions due to the left–right symmetry of the insertion optics.

A clear separation between the two categories is observed. Options 2 and 3, which pair magnets with large TF differences, produce $\langle\Delta\beta_{x,y}/\beta_{x,y}\rangle \in [3.5\%, 4.5\%]$ and peak values reaching 8–9%. Options 1 and 4, by contrast, feature uniform $\langle\Delta\beta_{x,y}/\beta_{x,y}\rangle \in [1\%, 2\%]$, with maximum excursions remaining below $\sim$ 4%. Based on this analysis, Options 2 and 3 are discarded.

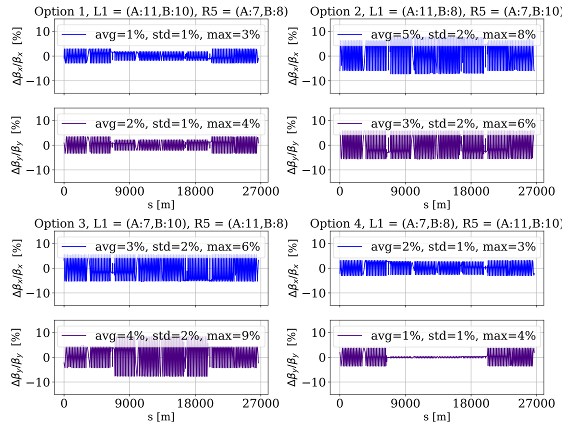

Figure 1: β-beating for Beam 1 for the four sorting options. Options 1 and 4 yield uniformly low β-beating ($\lesssim$ 4% peak), whereas Options 2 and 3 exhibit significantly larger values, with peaks of $\sim$ 8–9%.

AMPLITUDE DETUNING SORTING

To choose among the two remaining candidates, Options 1 and 4, the impact of b_4 can be adopted as a secondary sorting criterion. This strategy is motivated by the consideration that during the initial stage of the beam commissioning [22], when the non-linear corrector magnets will not be used, the quality of optics measurements and corrections, are based on AC dipole excitations that could be limited by the available forced Dynamic Aperture with large amplitude detuning [23].

The standard multipole expansion for the vertical field component (normal terms only) reads [24]:

$$B_y(x, y) = B_{\mathrm{main}} \left[\frac{b_2}{R_{\mathrm{ref}}} x + \frac{b_4}{R^3_{\mathrm{ref}}} (x^3 - 3xy^2) + \cdots \right], \quad (1)$$

where b_n are the multipole coefficients normalised to the main field at the reference radius R_{ref}) and B_{main} is the component of the main field.

The integrated octupolar strength associated with a quadrupolar integrated strength $K_1 L = B_{\mathrm{main}}\, b_2\, L/R_{\mathrm{ref}}$ is:

$$K_3 L = \frac{3!\, b_4\, K_1 L}{R^2_{\mathrm{ref}}}\,. \quad (2)$$

Equation (2) is used to convert the measured values b_4 from Table 1 into equivalent octupolar kicks in the simulation, placed at the location of the corresponding Q2 magnet. The b_4 values are expressed in units (1 unit = 10^{-4}).

These kicks produce an amplitude detuning defined as:

$$\Delta Q_x = a_{xx}\, J_x + a_{xy}\, J_y\,, \qquad \Delta Q_y = a_{xy}\, J_x + a_{yy}\, J_y\,. \quad (3)$$

The detuning coefficients are evaluated both analytically and via 4D tracking simulations, exhibiting agreement at the sub-percent level.

To condense the comparison into a single scalar observable, we define the norm of the detuning matrix $\mathbf{D}$,

$$\mathbf{D} = \begin{pmatrix} a_{xx} & a_{xy} \\ a_{xy} & a_{yy} \end{pmatrix}, \qquad \|\mathbf{D}\| = \sqrt{a^2_{xx} + a^2_{yy} + 2\, a^2_{xy}}\,, \quad (4)$$

as the value for ranking the remaining options. In particular, having to optimise the lattice for both beams simultaneously, we minimise $\|\mathbf{D}_{\mathrm{B1,B2}}\| = \sqrt{\|\mathbf{D}_{\mathrm{B1}}\|^2 + \|\mathbf{D}_{\mathrm{B2}}\|^2}$.

To place Options 1 and 4 in a broader context, it is instructive to relax all pairing and position constraints and consider the full space of possible Q2 assignments. Lifting the restriction that the Q2A and Q2B types must be preserved, all $8! = 40\,320$ permutations of the eight MQXFB magnets are evaluated in the eight available slots.

The result is shown in Fig. 2, where $\|\mathbf{D}_{\mathrm{B1}}\|$ is plotted against $\|\mathbf{D}_{\mathrm{B2}}\|$ for all permutations. A striking feature of the distribution is that all points collapse onto a 1D line instead of filling a 2D region. This behaviour is a direct consequence of the left–right symmetry of the HL-LHC insertion regions optics, i.e. β_x of Beam 1 is identical to β_y of Beam 2 on each side of the IP.

The global minimum for the detuning effects lies at $\|\mathbf{D}_{\mathrm{B1,B2}}\| \approx 1.1 \times 10^5\,\mathrm{m}^{-1}$. Option 4 is found to be close to this global optimum, with $\|\mathbf{D}_{\mathrm{B1,B2}}\| = 1.23 \times 10^5\,\mathrm{m}^{-1}$. Option 1, instead, yields $\|\mathbf{D}_{\mathrm{B1,B2}}\| = 2.47 \times 10^5\,\mathrm{m}^{-1}$, placing it roughly in the middle of the full distribution. From an amplitude-detuning standpoint alone, Option 4 would therefore be preferable by a factor of ~ 2. However, when the study was completed, the Q2Bs magnets already had fixed slots, so the only feasible option was Option 1.

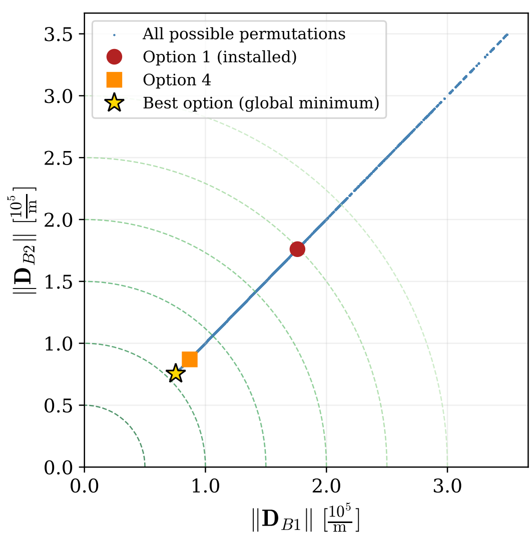

Figure 2: Norm of the amplitude detuning $\|\mathbf{D}_{\mathrm{B2}}\|$ vs. $\|\mathbf{D}_{\mathrm{B1}}\|$ for all unconstrained permutations of the eight MQXFB magnets into the eight Q2 slots. Iso-norm contours of $\|\mathbf{D}_{\mathrm{B1,B2}}\|$ are shown as dashed circles. The installed assignment (Option 1) and the b_4-optimal constrained option (Option 4) are highlighted, together with the global minimum.

SCHEDULING CONSTRAINTS

The studies presented above are based on the final Q2 magnet inventory. The limited sample size, only eight MQXFB units in total, makes any sorting algorithm inherently sensitive to changes in that inventory.

An instructive example of this sensitivity emerged when the discovery of a nonconformity led to the withdrawal of MQXFB09 and its replacement by the spare unit, i.e. MQXFB11. The studies originally presented at the 15th HL-LHC Collaboration Meeting [25] and in a subsequent follow-up [26], which were carried out with the original inventory, including MQXFB09, identified a different pair of optimal options (namely Options 2 and 3). This discrepancy with the present findings is entirely attributable to the low statistics: with only four magnets to sort, even a single substitution reshuffles the relative TF and b_4 deviations sufficiently to alter the final ranking of the available options. This underlines the fragility of sorting algorithms applied to very small samples of magnets and the necessity of re-evaluating the sorting whenever the magnet inventory evolves.

On the other hand, the methodology itself is robust: the two-stage approach, first discarding options with large TF imbalances to limit β-beating, then using FQ-driven amplitude detuning to choose among the remaining options, remains applicable irrespective of the specific magnet set.

Hence, as a result of our studies, the sorting for the last four HL-LHC Q2 magnets is the following: MQXFB07 (Q2A) and MQXFB08 (Q2B) at R5, MQXFB11 (Q2A) and MQXFB10 (Q2B) at L1.

CONCLUSIONS

A systematic sorting strategy for the HL-LHC Q2 magnets (MQXFB) has been presented, combining TF and FQ criteria in a two-stage approach.

Full lattice simulations performed with Xsuite demonstrate that the four candidate sorting configurations separate into two well-defined classes on the basis of TF-induced β-beating. Configurations pairing magnets with similar TF values (Options 1 and 4) produce uniform β-beating of $\sim$ 1–2%, while those pairing magnets with disparate TF values (Options 2 and 3) reach average values of up to $\sim 4.6\%$. A secondary discrimination between the two remaining options is provided by the amplitude detuning generated by the measured b_4 octupolar errors, evaluated both analytically and by 4D tracking. An exhaustive scan over all unconstrained permutations of the eight magnets revealed that the left–right symmetry of the HL-LHC insertion optics constrains the full distribution to a 1-D locus in the $(\|\mathbf{D}_{\mathrm{B1}}\|, \|\mathbf{D}_{\mathrm{B2}}\|)$ plane.

A central observation of this work is the pronounced sensitivity of the sorting outcome to the magnet inventory when the sample size is small. Indeed, replacing a single unit, MQXFB09, with a spare, MQXFB11, was sufficient to reverse the original option ranking. However, the methodology developed here is currently being extended to the Q1 and Q3 magnets, with the ultimate objective of achieving an optimised sorting of the full HL-LHC inner triplet.

ACKNOWLEDGEMENTS

We thank our colleagues of the HL-LHC WP2 and WP3 for their input and contributions to this study.

REFERENCES

[1] M. Li and S. Ohnuma, "Two-Parameter Sorting of Dipoles in Large Synchrotrons", in *Proc. EPAC'90*, Nice, France, Jun. 1990, pp. 1175–1178.

[2] V. Ziemann, "Sorting the LHC Dipoles using Simulated Annealing", in *Proc. EPAC'94*, London, UK, Jun.-Jul. 1994, pp. 1054–1057.

[3] M. Giovannozzi, R. Grassi, W. Scandale, and E. Todesco, "Sorting approach to magnetic random errors", *Phys. Rev. E*, vol. 52, no. 3, pp. 3093–3101, Sep. 1995. doi:10.1103/PhysRevE.52.3093

[4] D. Dinev, "Magnet Sorting Algorithms", in *Proc. EPAC'96*, Sitges, Spain, paper TUP045G, pp. 1374–1376, Sep. 1996.

[5] R. Bartolini, W. Scandale, M. Giovannozzi, and E. Todesco, "Sorting Strategies for the CERN-LHC Dipoles", in *Proc. PAC'97*, Vancouver, Canada, May 1997, paper 2V034, pp. 1469–1471.

[6] C. H. Chang, T. C. Fan, I. Hsu, C. S. Hwang, and C. Wang, "Magnet Sorting Algorithms for the SRRC EPU5.6", in *Proc. EPAC'98*, Stockholm, Sweden, paper MOP31G, pp. 2219–2221, Aug. 1998. https://jacow.org/e98/papers/MOP31G.pdf

[7] J. Wei *et al.*, "Real-World Sorting of RHIC Superconducting Magnets", in *Proc. PAC'99*, New York, NY, USA, Mar. 1999, paper THP95, pp. 3176–3178. https://jacow.org/p99/papers/THP95.pdf

[8] X. R. Resende and R. M. Dias, "Magnet Sorting Algorithm Applied to the LNLS EPU", in *Proc. EPAC'04*, Lucerne, Switzerland, paper MOPKF004, pp. 303–305, Sep. 2004. http://accelconf.web.cern.ch/e04/papers/MOPKF004.pdf

[9] D. Raparia, A. V. Fedotov, Y. Y. Lee, and J. Wei, "Dipole and Quadrupole Sorting for the SNS Ring", in *Proc. EPAC'04*, Lucerne, Switzerland, paper TUPLT189, pp. 1574–1576, Sep. 2004. http://accelconf.web.cern.ch/e04/papers/TUPLT189.pdf

[10] S. Peggs, E. Laface, E. Sargsyan, and R. Zeng, "Sorting in the ESS", in *Proc. IPAC'14*, Dresden, Germany, Jun. 2014, pp. 3329–3331. doi:10.18429/JACoW-IPAC2014-THPME047

[11] Y. Peng, J. Pan, and J. X. Zhou, "Study on magnets sorting for the HEPS booster", in *Proc. IPAC'23*, Venice, Italy, pp. 1088–1090, Sep. 2023. doi:10.18429/JACoW-IPAC2023-MOPM044

[12] S. D. Fartoukh, "Installation Strategy for the LHC Main Dipoles", in *Proc. EPAC'04*, Lucerne, Switzerland, paper WEOALH03, pp. 176–178, Sep. 2004. http://accelconf.web.cern.ch/e04/papers/WEOALH03.pdf

[13] P. Bestmann *et al.*, "Magnet Acceptance and Allocation at the LHC Magnet Evaluation Board", no. 22, pp. 3739–3741, Aug. 2007. https://jacow.org/p07/papers/FROAKI01.pdf

[14] S. Fartoukh and M. Giovannozzi, "Dynamic aperture computation for the as-built CERN Large Hadron Collider and impact of main dipoles sorting", *Nucl. Instrum. Methods Phys. Res., A*, vol. 671, pp. 10–23, 2011. doi:10.1016/j.nima.2011.12.052

[15] A. Lombardi and Y. Papaphilippou, "Sorting strategies for the arc quadrupoles of the LHC", 2006. https://cds.cern.ch/record/972661

[16] O. Aberle *et al.*, "High-Luminosity Large Hadron Collider (HL-LHC): Technical design report", CERN, Geneva, Switzerland, 2020. doi:10.23731/CYRM-2020-0010

[17] T. Pugnat, A. Wegscheider, E. Todesco, M. Giovannozzi, and R. Tomas, "Sorting strategies for the new superconducting magnets for the CERN HL-LHC", in *Proc. IPAC'24*, Nashville, TN, USA, pp. 3003–3006, Jul. 2024. doi:10.18429/JACoW-IPAC2024-THPC16

[18] A. Fornara *et al.*, "HL-LHC magnets field quality: current situation, strategies and mitigation measures", presented at IPAC'26, Deauville, France, May 2026, paper WEP5069, this conference.

[19] O. Brüning and L. Rossi, *The High Luminosity Large Hadron Collider*, O. Brüning, Ed. World Scientific, 2024. doi:10.1142/13487

[20] *HL-LHC Lattice Version 19*, CERN, https://gitlab.cern.ch/acc-models/acc-models-lhc/-/tree/hl19, 2026.

[21] G. Iadarola *et al.*, "Xsuite: an integrated beam physics simulation framework", in *Proc. IPAC'24*, Nashville, TN, pp. 2623–2626, May 2024. doi:10.18429/JACoW-IPAC2024-WEPR56

[22] E. H. Maclean *et al.*, "New approach to LHC optics commissioning for the nonlinear era", *Phys. Rev. Accel. Beams*, vol. 22, no. 6, p. 061004, Jun. 2019. doi:10.1103/PhysRevAccelBeams.22.061004

[23] F. S. Carlier, R. Tomás, E. H. Maclean, and T. H. B. Persson, "First experimental demonstration of forced dynamic aperture measurements with LHC ac dipoles", *Phys. Rev. Accel. Beams*, vol. 22, no. 3, p. 031002, Mar. 2019. doi:10.1103/PhysRevAccelBeams.22.031002

[24] S. Turner, "CAS - CERN Accelerator School: 5th General Accelerator Physics Course", CERN, Geneva, Switzerland, 1994. doi:10.5170/CERN-1994-001

[25] A. Fornara, M. Giovannozzi, and G. Sterbini, "Results of sorting studies of the last four Q2 magnets", in *Proceedings of the 15th HL-LHC Collaboration Meeting*, Oct. 2025. https://indico.cern.ch/event/1559978/contributions/6664939/

[26] A. Fornara, M. Giovannozzi, and G. Sterbini, "Update on sorting of MQXB (based on b4)", in *HiLumi Special Joint WP2/WP3 Meeting*, Oct. 2025. https://indico.cern.ch/event/1602987/#31-update-on-sorting-of-mqxb-b